RESEARCH MEMORANDUM

EXPERIMENTAL INVESTIGATION OF THE DAMPING IN ROLL OF CRUCIFORM TRIANGULAR WING-BODY COMBINATIONS AT MACH NUMBERS FROM 1.5 TO 6.0

By Alfred G. Boissevain

Ames Aeronautical Laboratory
Moffett Field, Calif.

NATIONAL ADVISORY COMMITTEE
FOR AERONAUTICS

WASHINGTON

April 7, 1954

NATIONAL ADVISORY COMMITTEE FOR AERONAUTICS

RESEARCH MEMORANDUM

EXPERIMENTAL INVESTIGATION OF THE DAMPING IN ROLL OF CRUCIFORM TRIANGULAR WING-BODY COMBINATIONS AT MACH NUMBERS FROM 1.5 TO 6.0

By Alfred G. Boissevain

SUMMARY

Measurements have been made of the damping in roll of cruciform triangular wings of aspect ratios 0.64, 1.28, and 2.31 at supersonic Mach numbers from 1.5 to 6.0. The data were obtained by launching models from rifled guns and analyzing the time history of the model roll position in free flight.

Linear theory, modified for wing-wing interference in the presence of the body and for wing-body interference, is shown to be in good agreement with experiment at values of the reduced aspect ratio, βA, below about 2.5 and in fair agreement at values of βA above 4.0. A severe disagreement between theory and experiment occurs near a βA of 4.0 where the Mach number normal to the wing leading edge is transonic, similar to the usual free-stream transonic Mach number effects on rectangular wings. The damping-in-roll data of the present tests are in fair agreement with wind-tunnel data from other facilities but are appreciably higher in magnitude when compared to data from free-flight rocket-powered test vehicles.

INTRODUCTION

The damping-in-roll coefficient is one of the more important parameters affecting the dynamic stability of aircraft. The damping in roll of triangular wings in supersonic flow has been the subject of extensive theoretical investigations, references 1 to 6. These studies indicate that for airfoils of vanishing thickness, the variation of the reduced damping-in-roll coefficient, βC_{l_p}, is a unique function of the reduced aspect ratio, βA. The development of the theory is rather complete in that a single wing with and without a body and cruciform wings without

a body have been treated. It should be pointed out, however, that this theory does not predict effects of airfoil section or thickness.

The experimental evaluation of the theory has, for the most part, been confined to Mach numbers below 2 and values of βA less than 4 (subsonic Mach numbers normal to the wing leading edge). A comparison of the results of these experimental investigations (refs. 7 to 13) shows rather poor correlation among the experimental curves, although a spread of ±10 percent centered at 80 percent of theory would encompass the majority of the data.

A series of tests, which are the subject of this report, have been performed to determine the effects of changing the test Mach number and the wing aspect ratio on the applicability of the theory for an otherwise fixed wing-body configuration. A further aim of the present investigation was to extend the coverage of experimental data to values of βA above 4 (supersonic Mach numbers normal to the wing leading edge) and to Mach numbers as high as 6.0.

These tests were performed in the Ames supersonic free-flight wind tunnel on wings of three aspect ratios at Mach numbers from 1.5 to 6.0. The Reynolds number, based on the wing mean aerodynamic chord, varied from 0.5 to 4.5 million.

SYMBOLS

a_1, a_2	boundary constants in roll equation
A	aspect ratio, $\frac{b^2}{S/2}$
b	wing span, ft
C_l	rolling-moment coefficient, $\frac{\text{rolling moment}}{qSb}$
C_{l_p}	damping-in-roll coefficient, $\frac{dC_l}{d\frac{pb}{2V}}$
c	constant used in roll equation
d	body diameter, ft
I_X	axial moment of inertia of model, slug-ft^2
L_p	rolling moment due to rolling velocity, ft-lb/radian/sec

[redacted]

[redacted]

L_o	rolling moment due to asymmetry, ft-lb
M	Mach number
p	rolling velocity, radians/sec
$\frac{pb}{2V}$	helix angle generated by wing tip in roll, radians
q	dynamic pressure, lb/sq ft
S	total area of all four wing panels, including area inside body, sq ft
τ	time, sec
$\left(\frac{t}{c}\right)_{root}$	thickness-chord ratio of wing root chord
$\left(\frac{t}{c}\right)_{tip}$	thickness-chord ratio of wing tip chord
V	velocity of model with respect to air stream, ft/sec
β	$\sqrt{M^2-1}$
βA	reduced aspect ratio
ρ	air density, slugs/cu ft
φ	roll angle, radians

APPARATUS, TECHNIQUE, AND MODELS

Facility

The investigation was conducted in the Ames supersonic free-flight wind tunnel which is a short ballistics range inside a variable-pressure, Mach number 2, blowdown wind tunnel. The models are launched from guns mounted in the diffuser and travel upstream through the 15-foot-long test section. Details of the facility are given in reference 14.

[redacted]

Technique

The data were obtained from measurements of the model roll position as a function of time. Rifled 20 mm and 37 mm guns were used to launch the models at a high initial rate of roll (300 to 1200 rps). The roll angle was recorded by a camera, mounted on the model catcher in the wind-tunnel settling chamber, taking high-speed motion pictures (5000 frames per second) of the oncoming model silhouetted against the reflector of an electric arc searchlight. The time standard was simultaneously recorded on the edge of the film. The arrangement of the equipment used for the present test is shown in figure 1. Figure 2 is a portion of a typical film record showing successive frames and timing marks. In the four frames shown, the model roll attitude changed by about 45°, corresponding to a roll velocity of about 200 revolutions per second. The round object above and to the left of the model is the sabot base used in launching the model which, because of its higher drag, travels several feet behind the model in the test section. Values of φ as a function of time were obtained from film records such as the one shown.

Models

The models used in the present investigation, shown as a sketch in figure 3 giving over-all dimensions, and in a photograph (fig. 4), consisted of cone-cylinder bodies of fineness ratio 15 on which were mounted cruciform sweptback triangular wings acting as tail surfaces. The ratio of wing span to body diameter was 3.0. Three values of aspect ratio were tested, 0.64, 1.28, and 2.31, corresponding to sweepback angles of 81°, 72°, and 60°. The airfoil section parallel to the model axis was the same for all configurations, consisting of a flat plate with a symmetrical wedge leading edge and a blunt trailing edge. The included leading-edge wedge angle, 9.1°, was equivalent to that for a symmetrical double-wedge airfoil 8 percent thick. Because of the variation in sweep angle, the leading-edge wedge angle perpendicular to the wing leading edge varied between models of different aspect ratios, as shown in figure 3. The wings and that portion of the body supporting them were machined from aluminum alloy. The rest of the body was machined from either steel, aluminum, or magnesium alloy, depending on the longitudinal stability requirements.

The models shown in figures 3 and 4 were employed as standard models for purposes of the tests reported herein. The effect of certain modifications to several of the models was also investigated. Two aspect ratio 0.64 models were modified by reducing the leading-edge wedge angle normal to the wing leading edge from 53.7° to 29.4°. Several aspect ratio 1.28 and 2.31 models were modified by altering the surface condition of the wing leading edges, as shown in figure 5. Figure 5(a) shows

the leading-edge condition of a standard model; whereas figures 5(b) and 5(c) show, respectively, the rough and smooth conditions for the wing leading edges of the modified models.

A photograph of an aspect ratio 1.28 model mounted in a launching sabot is shown as figure 6.

REDUCTION OF DATA

The data reduction was based on the method presented in reference 15 and is described in detail in reference 14. These references assume that the single degree of freedom equation of roll,

$$I_x \frac{d^2\varphi}{d\tau^2} = L_o + L_p p \tag{1}$$

describes the rolling motion of the models. This expression, when solved for φ in terms of the independent variable, τ, can be expressed as

$$\varphi = a_1 + p_e\tau + a_2 e^{-c\tau} \tag{2}$$

where p_e is the equilibrium rate of roll, a_1 and a_2 are constants of integration, and

$$c = -C_{l_p}\left(\frac{b}{2V}\right)\frac{qSb}{I_x}$$

An effort was made to use equation (2) to reduce the data of this investigation. A few trials showed that satisfactory fitting of the data could be achieved with values of p_e and c varying over an unacceptably large range. The explanation for this follows from a consideration of equation (1). This equation shows that to find the total rolling moment acting on the model, $L_o + L_p p$, the data for φ as a function of τ must be differentiated twice. If L_o and $L_p p$ are to be separated, it amounts to solving a pair of simultaneous equations which contain two distinct values of the roll acceleration. In effect, the third derivative of φ with respect to τ must be known. The data were not precise enough to give this information because of the short length of the test range. If, however, the rolling moment due to asymmetry, L_o, is assumed zero, the expression for roll angle simplifies to

$$\varphi = a_1 + a_2 e^{-c\tau} \tag{3}$$

[redacted]

and the present data are adequate. Therefore, equation (3) was used for analyzing the data of this investigation. Justification for assuming $L_o = 0$, and errors due to this assumption, are discussed in the following section.

Because of the redundancy of the data, a solution can be made for the constants a_1, a_2, and c by the method of least squares as described in reference 14. The curve of figure 7 is a plot of the computed variation of φ with τ as obtained from the optimum values of the constants for a representative run. A straight line is included for comparison to show the curvature of the line defined by the data.

ACCURACY

Because of the nature of the test, a realistic estimate of the accuracy of the data is possible only from a consideration of the consistency of the data. The assumption of model symmetry is believed to be the most important source of potential error. However, the fin misalinements were measured on a surface plate and found to be no more than a few ten-thousandths of an inch over the root chord. A systematic error in fin alinement of about 0.001 inch on all four panels would produce a 10-percent error in the damping in roll for the worst condition. Since the measured misalinement was much smaller than 0.001 inch and was not systematic, it is believed that this source of error is on the order of a few percent.

The probable errors in measurement of test conditions and model dimensions are listed below.

V	±1 percent
p	±0.1 percent
b	±0.1 percent
τ	±0.2 percent
S	±0.05 percent
I_x	±0.5 percent
φ	±0.015 radians

Since the models were flown in free flight, they experienced small oscillations in both pitch and yaw, usually less than 3°. The results of reference 16 indicate that angles of attack of this amplitude produce negligible rolling moments, regardless of roll position.

THEORETICAL CONSIDERATIONS

The solution for the damping-in-roll coefficient of a triangular wing in supersonic flow, based on linear theory, is given in reference 1

[redacted]

and is presented as the dotted curve in figure 8. The solution obtained by applying slender-body theory to the same problem (ref. 2) is presented as the dashed curve of figure 8. Both of these assume a planar wing with no body. The linear theory, modified in the manner described in the following paragraphs to correspond to a cruciform wing-body configuration is shown in figure 8 as the solid curve.

Presented in figure 9 are the correction factors applied to the linear theory to account for wing-body interference and for wing-wing interference in the presence of a body. The effect of adding a body to a set of planar wings is derived in reference 2 for the condition of βA less than 4 and in reference 3 for the condition of βA equal to or greater than 4. These theoretical results are presented in figure 9 as the curve of wing-body interference. The theoretical effect of adding extra wing panels is derived in reference 4 by use of slender-body theory and in reference 5 by use of linearized theory. The effect of adding a body at the same time is considered in reference 6 by use of slender-body theory. While a rigorous solution for the effect of the body on the wing-wing interference for the nonslender case is complicated, an approximate solution can easily be obtained. The affected areas of the adjacent wing panel are simply defined if it is assumed that the perturbations from the intersection of the wing leading edge and the body must travel along the surface of the body in a helical path, defined by the body radius and Mach angle, to the adjacent wing panel before they can affect it. These affected areas are then considered to be acting at 81-percent efficiency compared to an isolated planar wing (refs. 4 and 5) while the rest of the wing is assumed to act at 100-percent efficiency. A correction factor, based on the moment of the areas affected, is obtained and is presented in figure 9 as the curve of wing-wing interference. This factor is a unique function of βA for a given value of span to body diameter ratio.

RESULTS AND DISCUSSION

The complete results of the present investigation are presented in figures 10(a) through 10(c) as a series of plots of βC_{l_p} vs. βA. The curve of modified linear theory, presented previously in figure 8, is included in each of the plots for comparison. The fairing of the data for each aspect ratio was guided by the data for the other configurations, especially for the case of figure 10(a). Figure 10(d) is a collection of the faired experimental curves of figures 10(a) through 10(c), again including the curve of modified linear theory for comparison.

Comparison With Theory

The theory predicts the damping-in-roll coefficient with good accuracy at values of βA below about 2.5. Near a βA of 4 (transonic Mach

[redacted]

numbers normal to the wing leading edge), the difference between theory and experiment becomes marked. The behavior of the damping-in-roll coefficient in this vicinity shows a strong similarity to the variations in lift and damping in roll of rectangular wings near a free-stream Mach number of 1.0, and will be discussed later in some detail. At values of βA well above 4, the data are in fair agreement with theory.

The agreement which is obtained between experiment and theory is surprising when the differences between the actual and assumed flow fields are considered. Examination of the flow fields in the vicinity of the wings as recorded in shadowgraphs (fig. 11), shows the presence of shock waves of appreciable strength, instead of the infinitesimal disturbances allowed by linear theory. Detached shock waves occurred at βA greater than 4, even though theory calls for Mach lines to be swept behind the leading edge. These are effects of finite thickness which, perhaps fortuitously, did not cause the experimental damping in roll to deviate from theory.

To see if the agreement would be affected by a change in the airfoil section, the wedge angle normal to the leading edge was modified on two models with aspect ratio 0.64 wings. This angle was made equal to the corresponding angle on wing of aspect ratio 1.28, resulting in an angle roughly half the original. These models were tested at a βA of 2.8 (triangular data points of fig. 10(a)), the result of which showed no detectable change in the value of the damping.

Transonic Effects

When the data of the present tests are plotted against the Mach number normal to the wing leading edge, the curve of figure 12 is produced. Also shown in figure 12 are data from reference 17 on the damping in roll of rectangular and untapered 45° swept wings with an NACA 65A009 airfoil section and aspect ratio of 3.7. It is interesting to note that in spite of the wide range of free-stream Mach numbers represented by a given value of the abscissa, the damping-in-roll coefficient of all the wings show a marked reduction at transonic Mach numbers normal to the wing leading edge. The minimum values of the damping-in-roll coefficient all occur at Mach numbers normal to the wing leading edge between 0.90 and 1.00, corresponding to a free-stream Mach number of about 6.0 for the models of aspect ratio 0.64 and about 2.0 for the models of aspect ratio 2.31. The data known to the author on the damping in roll of triangular wings do not show any similar severe decrease in damping near βA of 4. However, the results of reference 18 showed that transonic shock conditions on triangular wings are similar to those occurring on rectangular wings in the usual transonic flow.

The thickness-to-chord ratio of the wings used in the present tests varied from 2.6 percent and 3.9 percent at the root chord to 16 percent at the tip because of the type of airfoil section used. It should be pointed out, however, that the wedge angle parallel to the air stream is equivalent to that for an 8-percent-thick double-wedge airfoil. It is probable that this high thickness-to-chord ratio at and near the tip was a contributing factor to these transonic effects since it is well known that thick airfoils show more severe transonic effects than do thin sections.

The fairing of the data curves in this region is not too well defined, except in the case of the aspect ratio 2.31 wing; however, there is an indication that for the wings of the present investigation, increasing the aspect ratio increases the severity of the loss in damping.

As is usual in transonic-flow problems, sensitivity to the nature of the flow in the boundary layer was found. In the case of the aspect ratio 1.28 wing, the boundary-layer character was altered by polishing or roughening the wing leading edge. The smooth and rough conditions are shown in figure 5. Unpublished experiments in the supersonic free-flight wind tunnel have indicated that for the Reynolds numbers and test conditions encountered in this tunnel, a leading edge notched in the manner shown in figure 5(b) will produce turbulence starting at the leading edge. The difference in damping produced by these variations is shown in figure 10(b). The effect of changing the boundary layer from laminar to turbulent is to reduce the damping-in-roll coefficient at values of βA slightly less than 4 and to increase it at values of βA above 4. This difference appears to be limited to the region of transonic flow normal to the wing leading edge. One point was obtained with a rough leading edge on the aspect ratio 2.31 model in this transonic range and showed no effect (fig. 10(c)). No effort was made to completely define this case.

Comparison With Other Facilities

Figure 13 compares the data of the present investigation and the collected data of references 7 to 13. The agreement of the present data and that of wind-tunnel tests, shown by individual points, is fair. The data of free-flight rocket-powered models lie generally low compared to the present data. It should be emphasized that in every case the data are compared with the linear-theory values for the particular configurations which were tested. For the two- and three-wing cases, the same basic concepts were used as those described for the cruciform case in the section on theory. The data of the present test and of references 7 to 13 were all obtained for the same range of wing-tip helix angles (0 to 0.07).

[redacted]

Systematic configurational differences were sought which could explain the observed variation in damping. For this purpose a more detailed comparison was made of the data for aspect ratio 2.31 wings. These data are shown in figure 14. A careful comparison of these data with the included chart of configurational details does not lead to any definite pattern of correlation. For example, a comparison of the data on the basis of the various airfoil sections used shows that there is better agreement between airfoils of dissimilar shape and thickness than for more closely related airfoils. A similar comparison on the basis of the ratio of wing span to body diameter, b/d, shows that the data for the configurations with the largest values of b/d agreed more closely with those for the lowest value of b/d than did tne data for the configurations with intermediate values of b/d. A study of the possible effect of other configurational differences, such as the number of wings, position of the wings on the body, and the body shape, showed similar inconsistences. Therefore, for the present, the differences in the damping cannot be explained on the basis of configurational differences alone. Aeroelastic effects due to differences in model construction and conditions of dynamic pressure under which the tests were made, as well as general differences in test techniques, might, in part, account for the observed differences in damping.

CONCLUDING REMARKS

Free-flight measurements have been made of the damping in roll of cruciform triangular wings at Mach numbers from 1.5 to 6.0. Linear theory, modified for wing-wing interference in the presence of a body and for wing-body interference, was found to be in good agreement with the data at values of βA below about 2.5. The agreement between theory and experiment is fair at values of βA above 4.0. There is a marked disagreement between theory and experiment near a βA of 4 (transonic Mach numbers normal to the wing leading edge). The variation of the damping-in-roll coefficient with transonic Mach numbers normal to the wing leading edge shows a marked similarity to the variation of the damping in roll of rectangular wings with free-stream transonic Mach numbers. In this same speed range, the models of aspect ratio 1.28 were sensitive to type of boundary-layer flow.

The data of the present tests were in fair agreement with wind-tunnel data obtained from spinning models, but were appreciably higher in magnitude when compared with data obtained from free-flight rocket-powered test vehicles. An effort to explain these differences in terms of configurational differences was unsuccessful.

Ames Aeronautical Laboratory
National Advisory Committee for Aeronautics
Moffett Field, Calif., Feb. 15, 1954

[redacted]

REFERENCES

1. Brown, Clinton E., and Adams, Mac C.: Damping in Pitch and Roll of Triangular Wings at Supersonic Speeds. NACA Rep. 892, 1948. (Formerly NACA TN 1566)

2. Lomax, Harvard, and Heaslet, Max. A.: Damping-in-Roll Calculations for Slender Swept-Back Wings and Slender Wing-Body Combinations. NACA TN 1950, 1949.

3. Tucker, Warren A., and Piland, Robert O.: Estimation of the Damping in Roll of Supersonic-Leading-Edge Wing-Body Combinations. NACA TN 2151, 1950.

4. Adams, Gaynor J.: Theoretical Damping in Roll and Rolling Effectiveness of Slender Cruciform Wings. NACA TN 2270, 1951.

5. Ribner, Herbert S.: Damping in Roll of Cruciform and Some Related Delta Wings at Supersonic Speeds. NACA TN 2285, 1951.

6. Adams, Gaynor J., and Dugan, Duane W.: Theoretical Damping in Roll and Rolling Moment Due to Differential Wing Incidence for Slender Cruciform Wings and Wing-Body Combinations. NACA Rep. 1088, 1952.

7. Sanders, E. Claude, Jr.: Damping in Roll of Models with 45°, 60°, and 70° Delta Wings Determined at High Subsonic, Transonic, and Supersonic Speeds with Rocket-Powered Models. NACA RM L52D22a, 1952.

8. Martz, William C., and Church, James C.: Flight Investigation at Subsonic, Transonic, and Supersonic Velocities of the Hinge-Moment Characteristics, Lateral-Control Effectiveness, and Wing Damping in Roll of a 60° Sweptback Delta Wing with Half-Delta Tip Ailerons. (Revised) NACA RM L51G18, 1951.

9. Bland, William M., Jr., and Sandahl, Carl A.: A Technique Utilizing Rocket-Propelled Test Vehicles for the Measurement of the Damping in Roll of Sting-Mounted Models and Some Initial Results for Delta and Unswept Tapered Wings. NACA RM L50D24, 1950.

10. Brown, Clinton E., and Heinke, Harry S., Jr.: Preliminary Wind-Tunnel Tests of Triangular and Rectangular Wings in Steady Roll at Mach Numbers of 1.62 and 1.92. NACA RM L8L30, 1949.

11. Bland, William M., Jr.: Effect of Fuselage Interference on the Damping in Roll of Delta Wings of Aspect Ratio 4 in the Mach Number Range Between 0.6 and 1.6 as Determined with Rocket Propelled Vehicles. NACA RM L52E13, 1952.

[redacted]

12. Beal, R. R.: Roll-Damping and Additional Roll-Control Characteristics of the Sparrow 14-B at M = 2.50 as Determined by Wind-Tunnel Tests of a 13-5-Percent-Scale Model. Douglas Aircraft Co. Rep. SM-14062, Dec. 18, 1951. BUAER, Navy Dept., Contract NOa(s)51-513.

13. McDearmon, Russell W., and Heinke, Harry S., Jr.: Investigation of the Damping in Roll of Swept and Tapered Wings at Supersonic Speeds. NACA RM L53A13, 1953.

14. Seiff, Alvin, James, Carlton S., Canning, Thomas N., and Boissevain, Alfred G.: The Ames Supersonic Free-Flight Wind Tunnel. NACA RM A52A24, 1952.

15. Bolz, Ray E., and Nicolaides, John D.: A Method of Determining Some Aerodynamic Coefficients from Supersonic Free Flight Tests of a Rolling Missile. Aberdeen Proving Ground, Aberdeen, Md., BRL Rep. 711, 1949. (Also issued in: I.A.S. Preprint 252, 1950)

16. McCabe, A. P.: Induced Rolling Moments on the NIKE and Sparrow Missiles. Douglas Aircraft Co. Rep. SM-13795, July 19, 1950.

17. Bland, William M., Jr., and Dietz, Albert E.: Some Effects of Fuselage Interference, Wing Interference, and Sweepback on the Damping in Roll of Untapered Wings as Determined by Techniques Employing Rocket-Propelled Vehicles. NACA RM L51D25, 1951.

18. Boyd, John W., and Phelps, E. Ray: A Comparison of the Experimental and Theoretical Loading Over Triangular Wings at Supersonic Speeds. NACA RM A50J17, 1951.

[redacted]

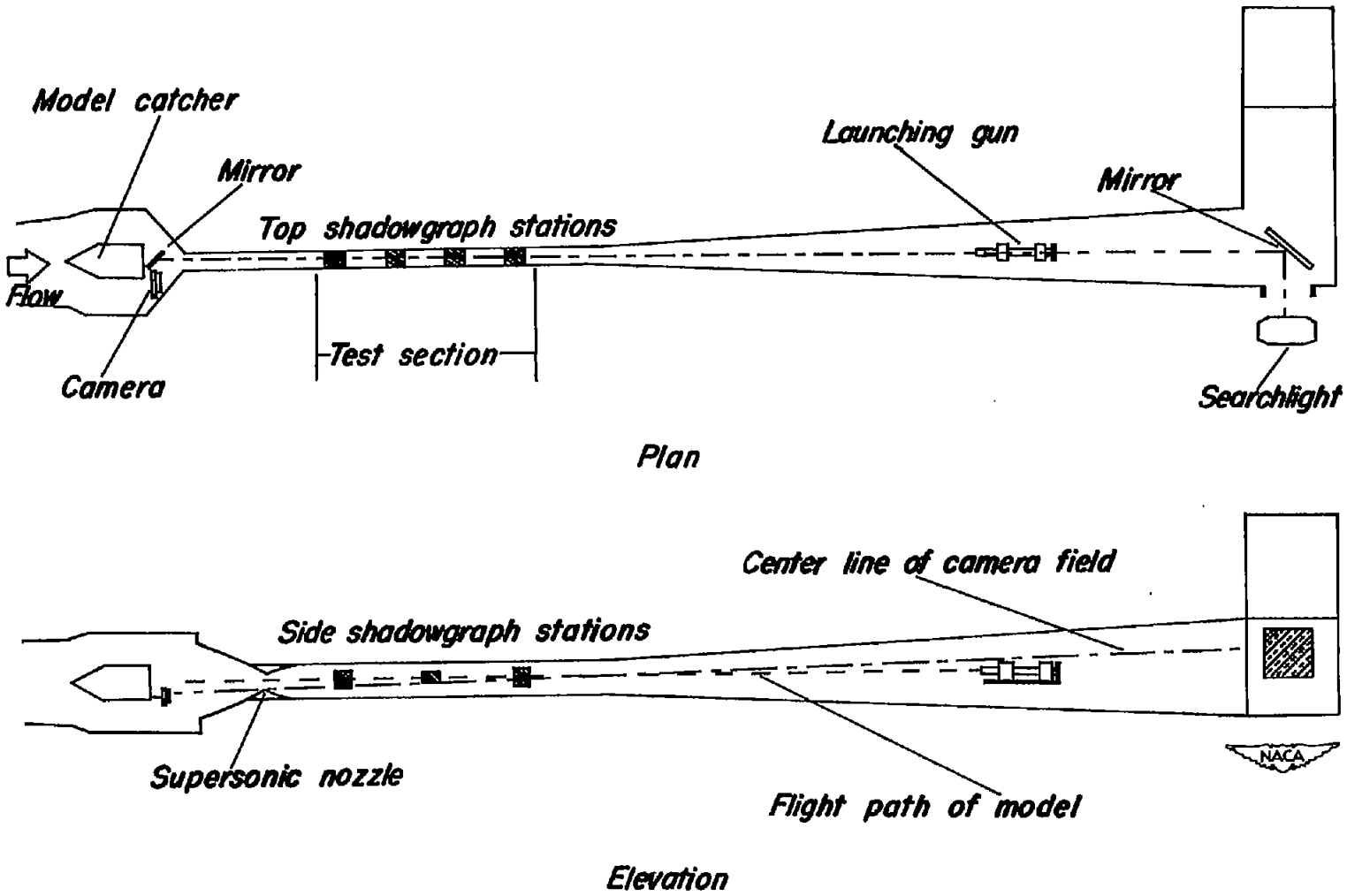

Figure 1 .- Sketch of the Ames supersonic free-flight wind tunnel showing arrangement of equipment for photographing roll position.

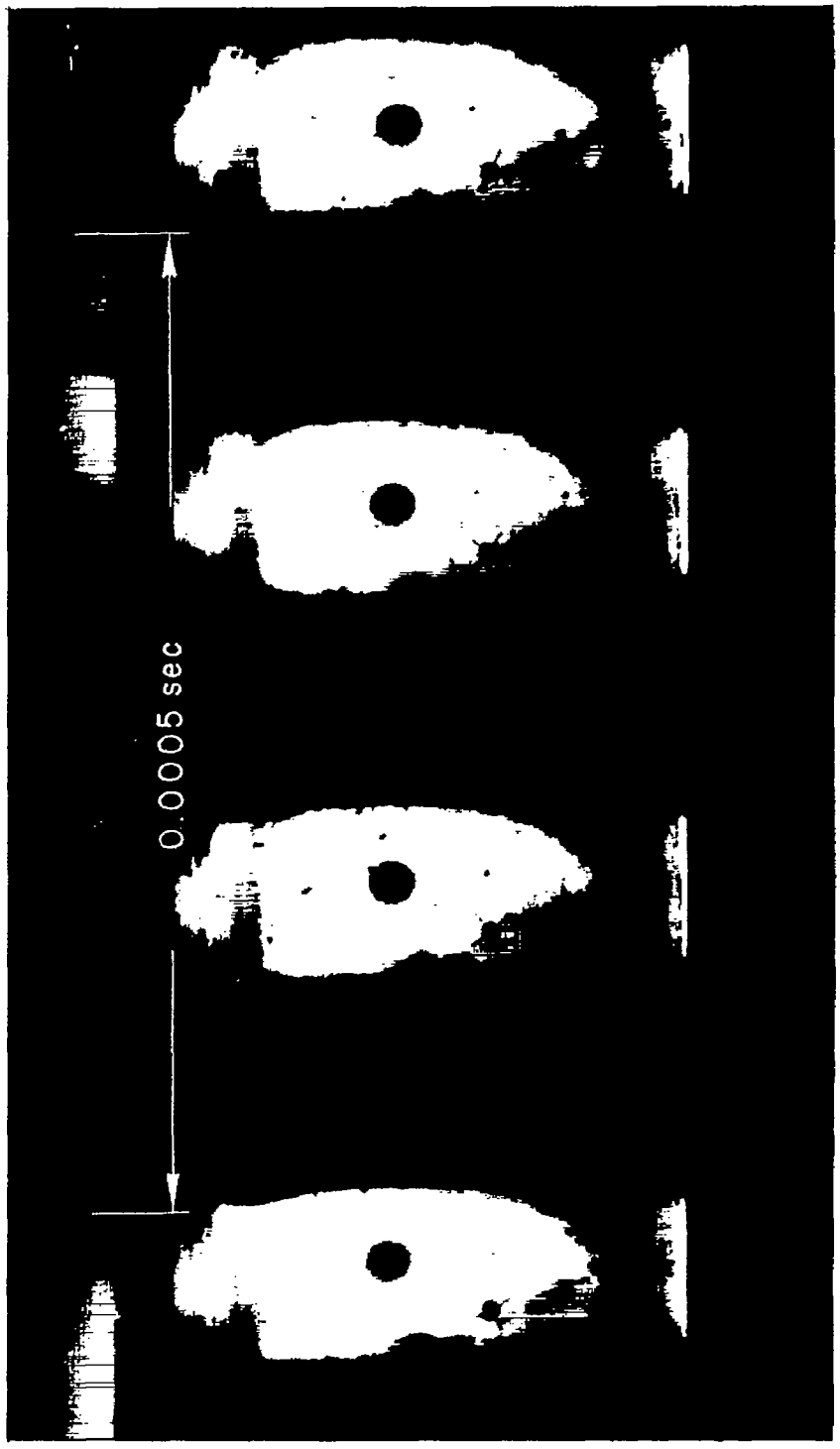

Figure 2.- Portion of film record of model roll position.

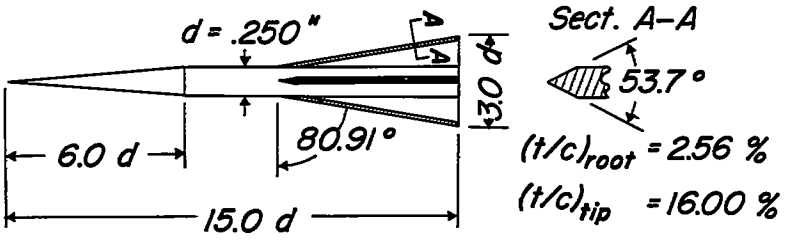

Aspect ratio 0.64

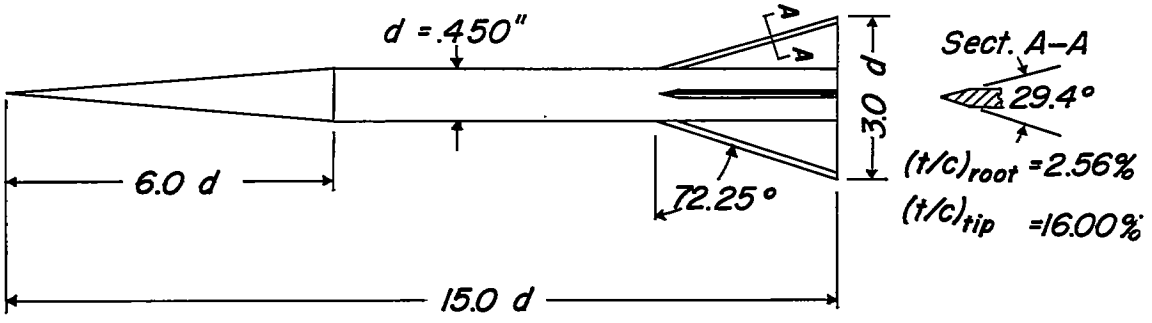

Aspect ratio 1.28

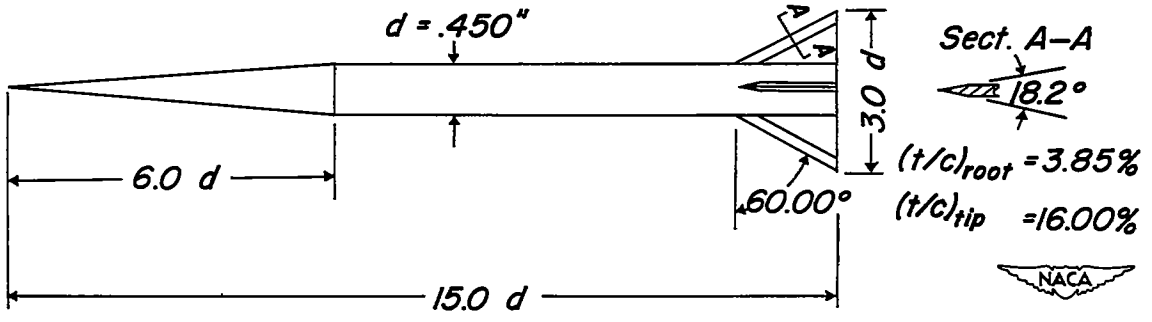

Aspect ratio 2.31

Figure 3.- Test configurations.

[redacted]

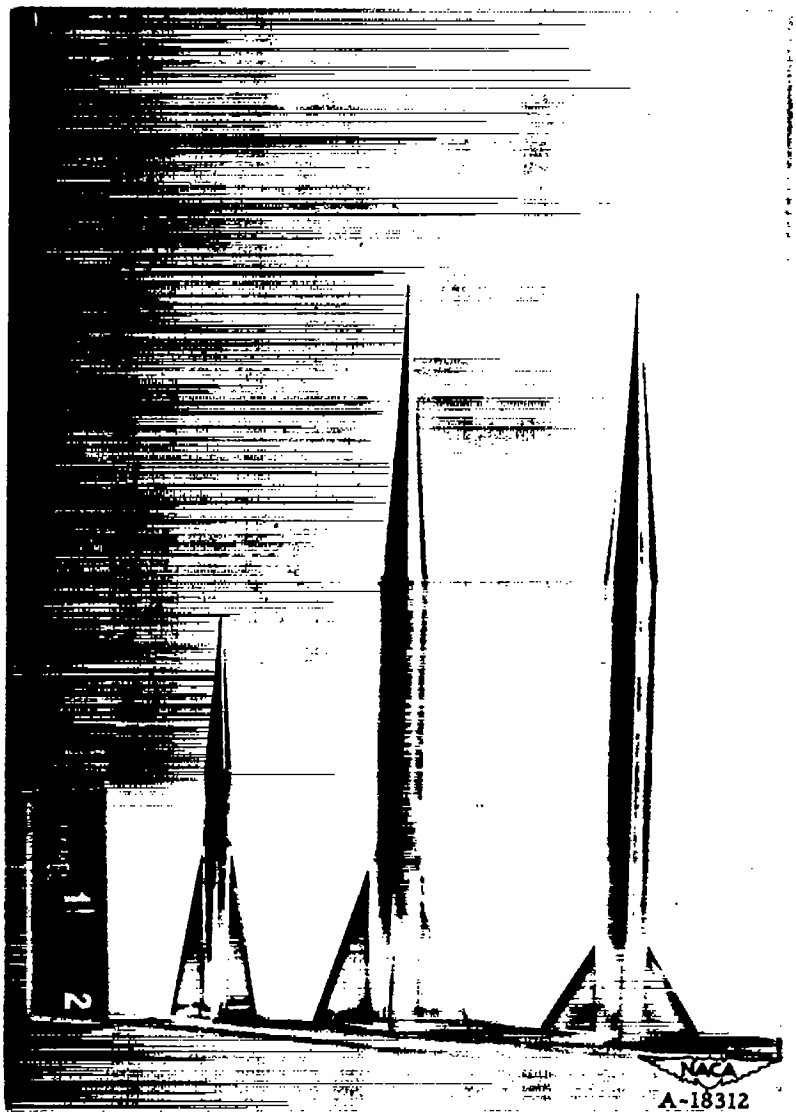

Figure 4.- Photograph of test configurations.

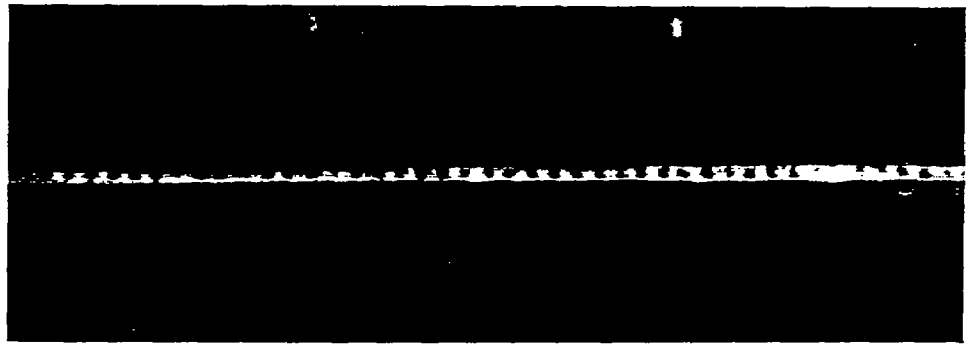

(a) Standard leading edge.

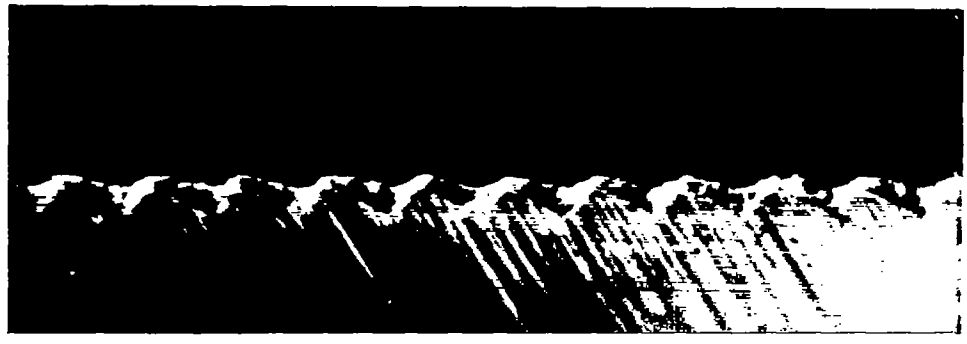

(b) Rough leading edge.

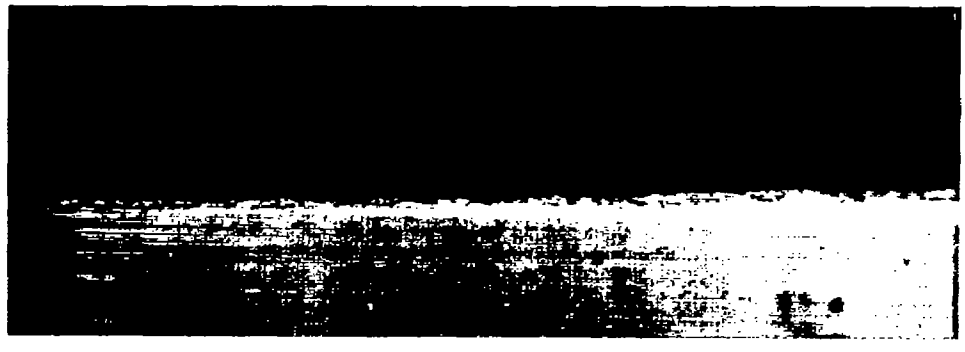

A-18821

(c) Smooth leading edge.

Figure 5.- Photographs at 54X magnification of leading-edge condition of model of aspect ratio 1.28.

[redacted]

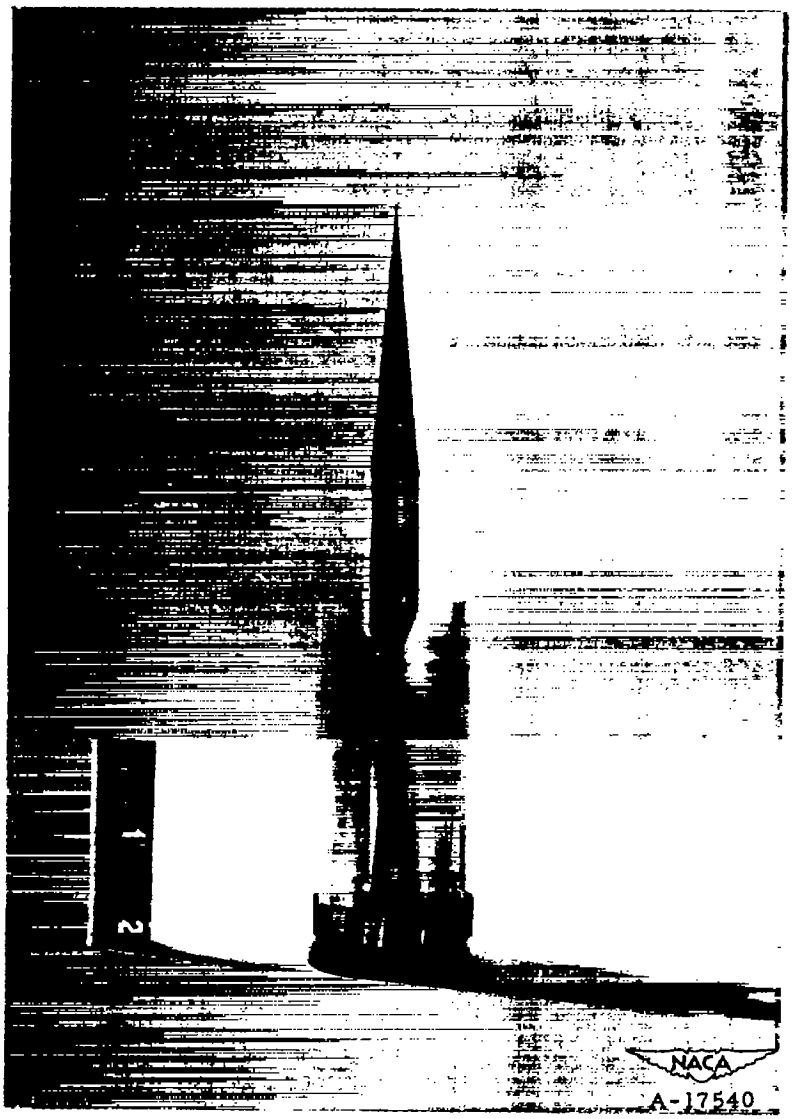

Figure 6.- Model of aspect ratio 1.28 with sabot assembled for launching.

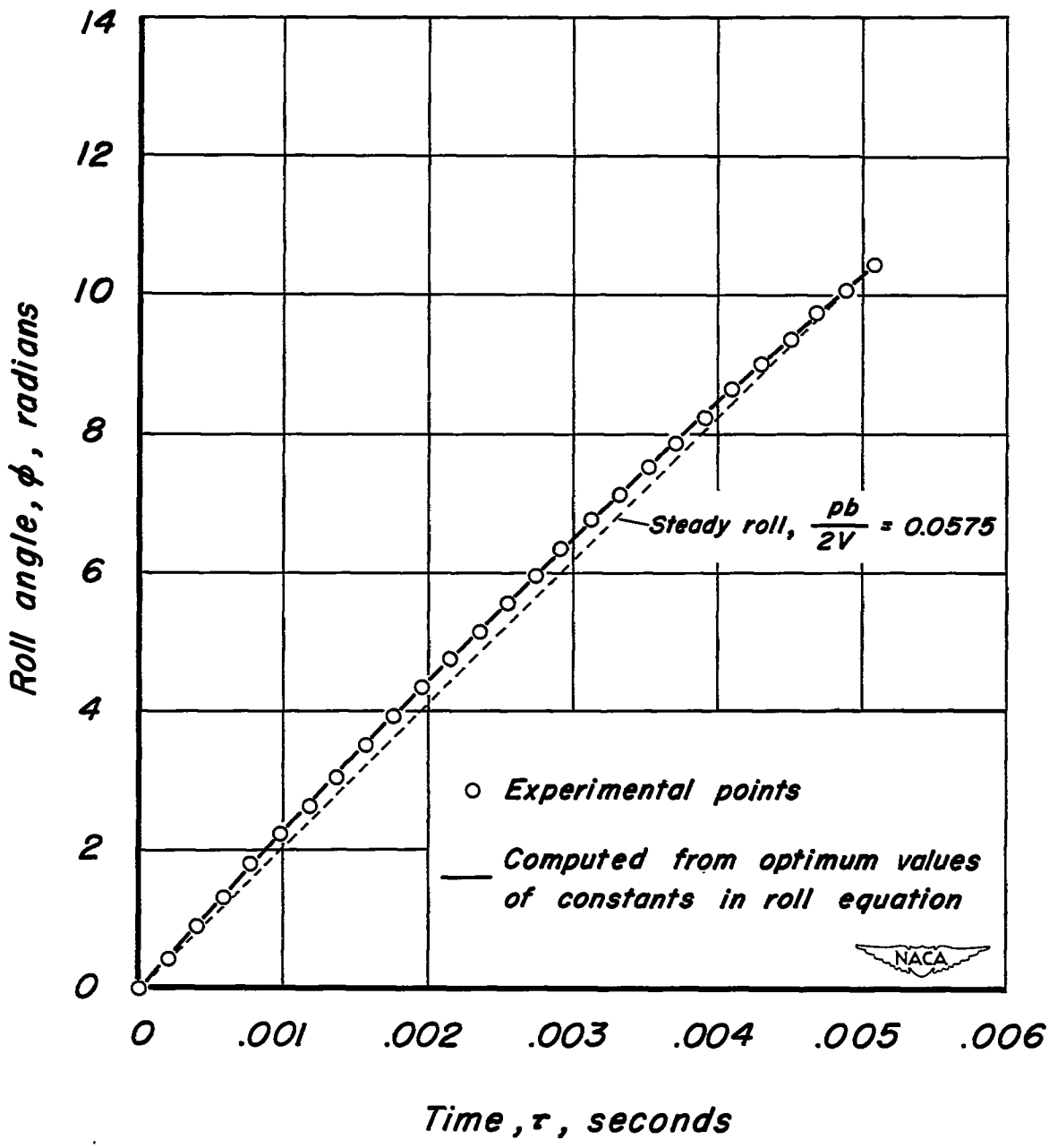

Figure 7.- Variation of model roll angle with time.

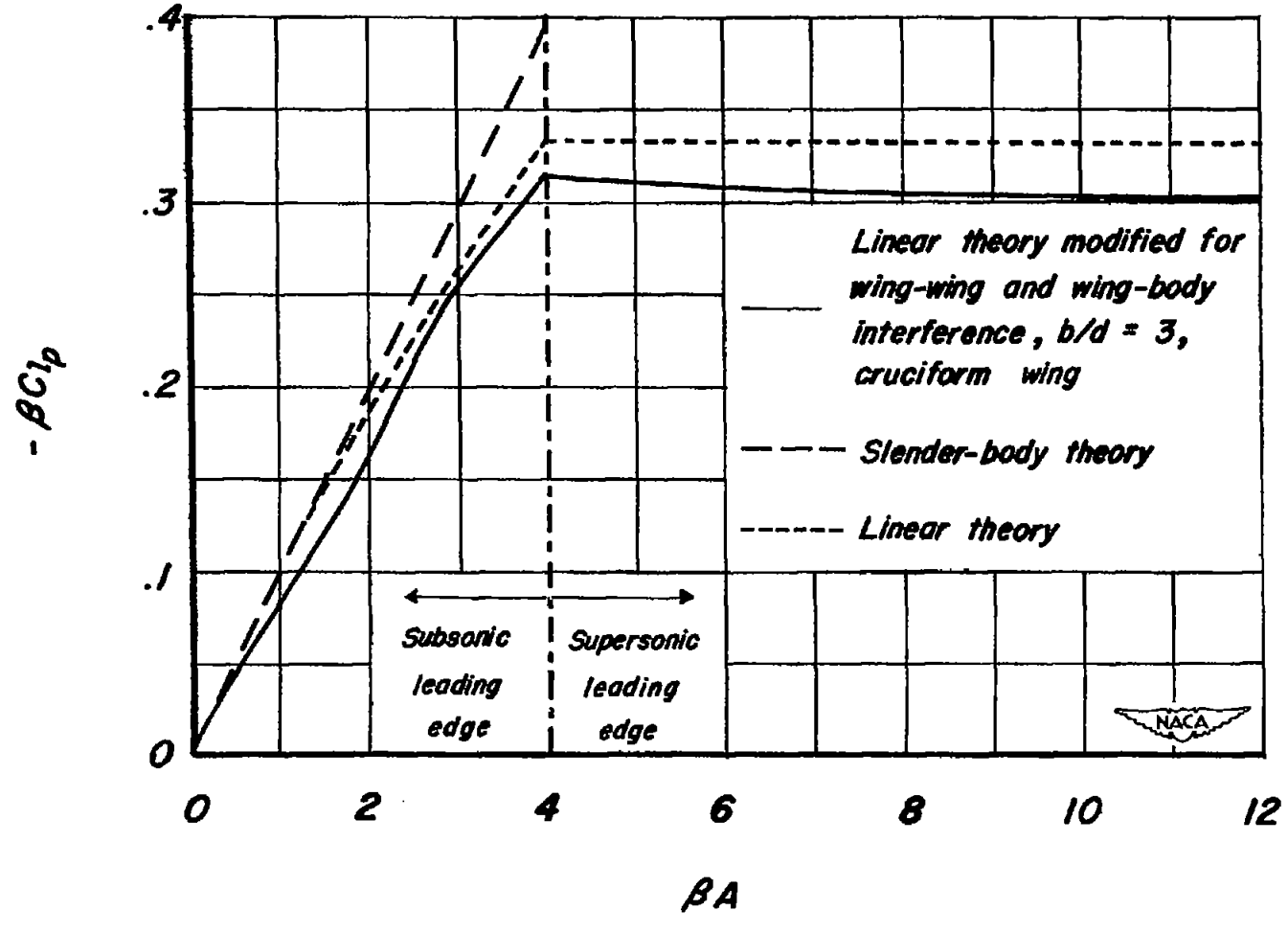

Figure 8.- Theoretical variation of reduced damping-in-roll coefficient with reduced aspect ratio.

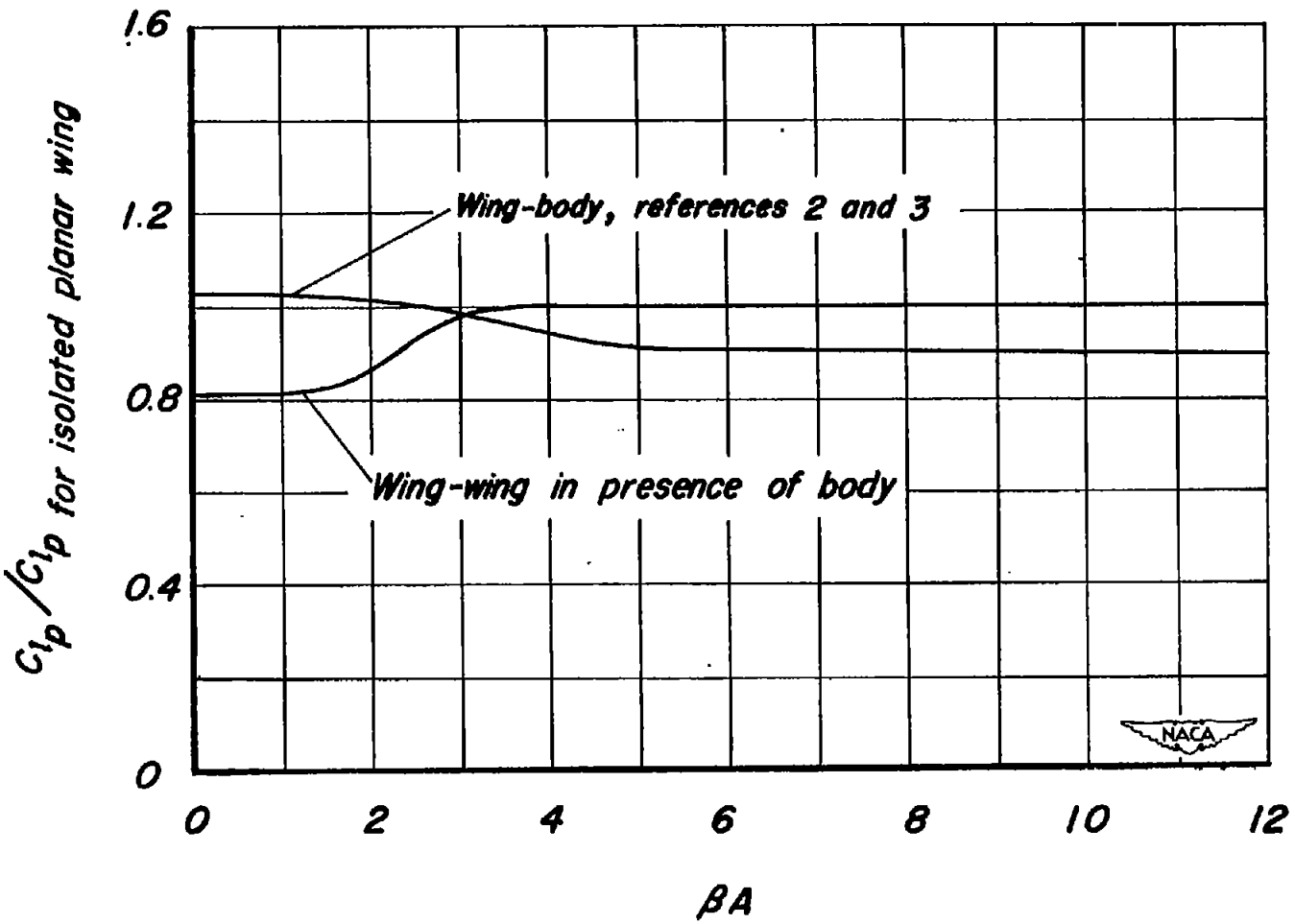

Figure 9.- Interference correction factors for cruciform triangular wing-body configuration of b/d = 3.

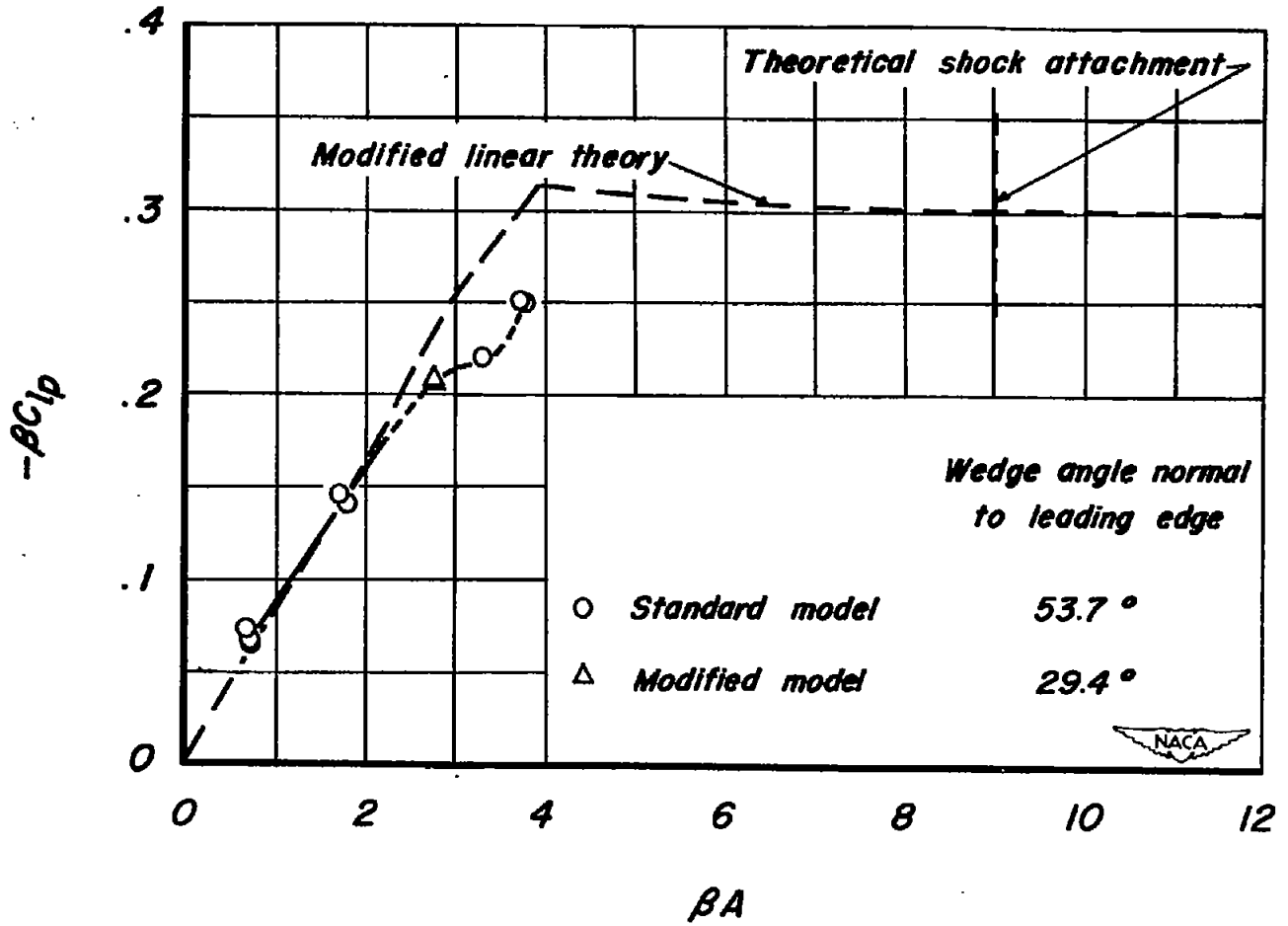

(a) Aspect ratio 0.64.

Figure 10.- Experimental variation of reduced damping-in-roll coefficient with reduced aspect ratio.

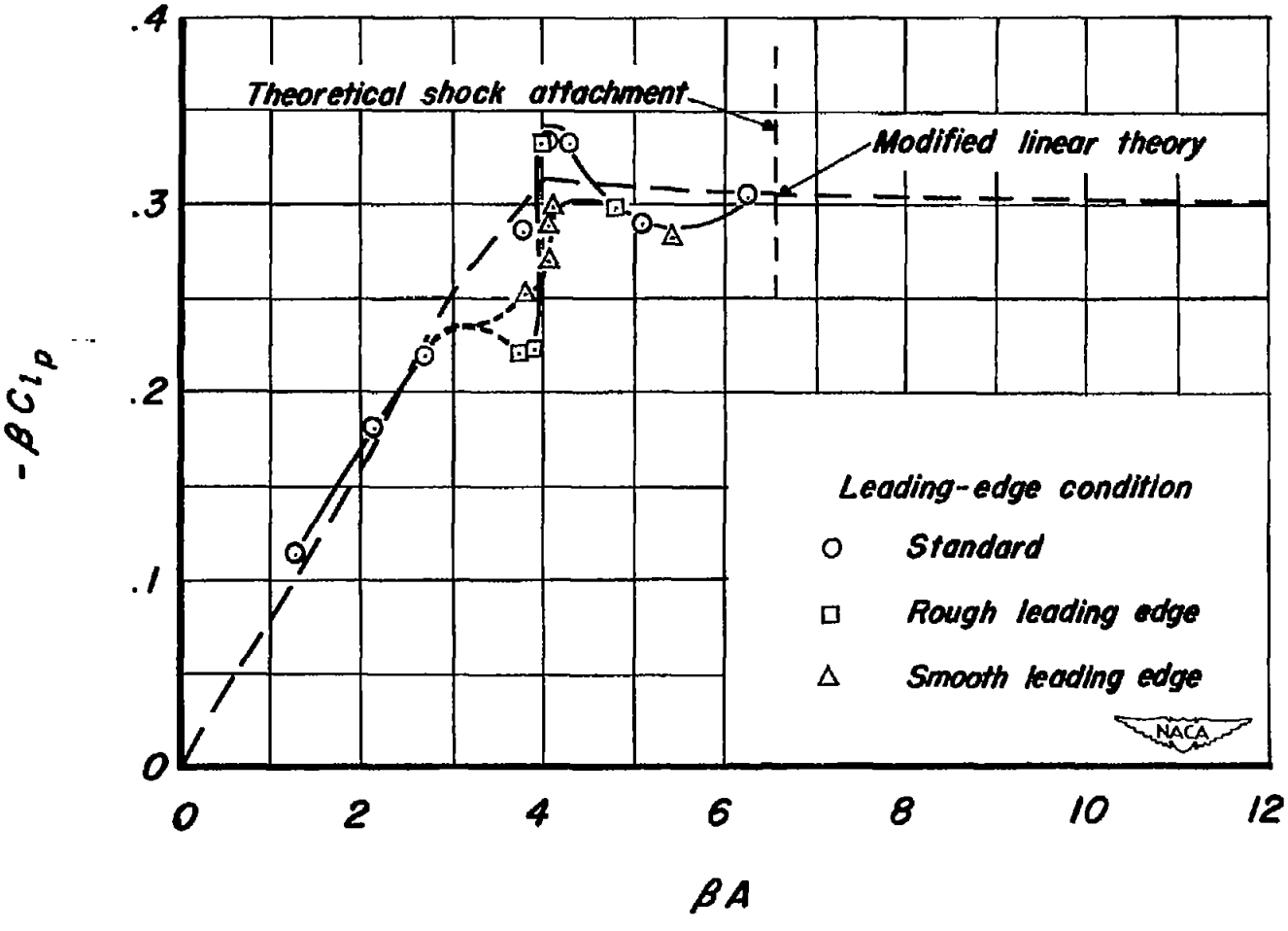

(b) Aspect ratio 1.28.

Figure 10.- Continued.

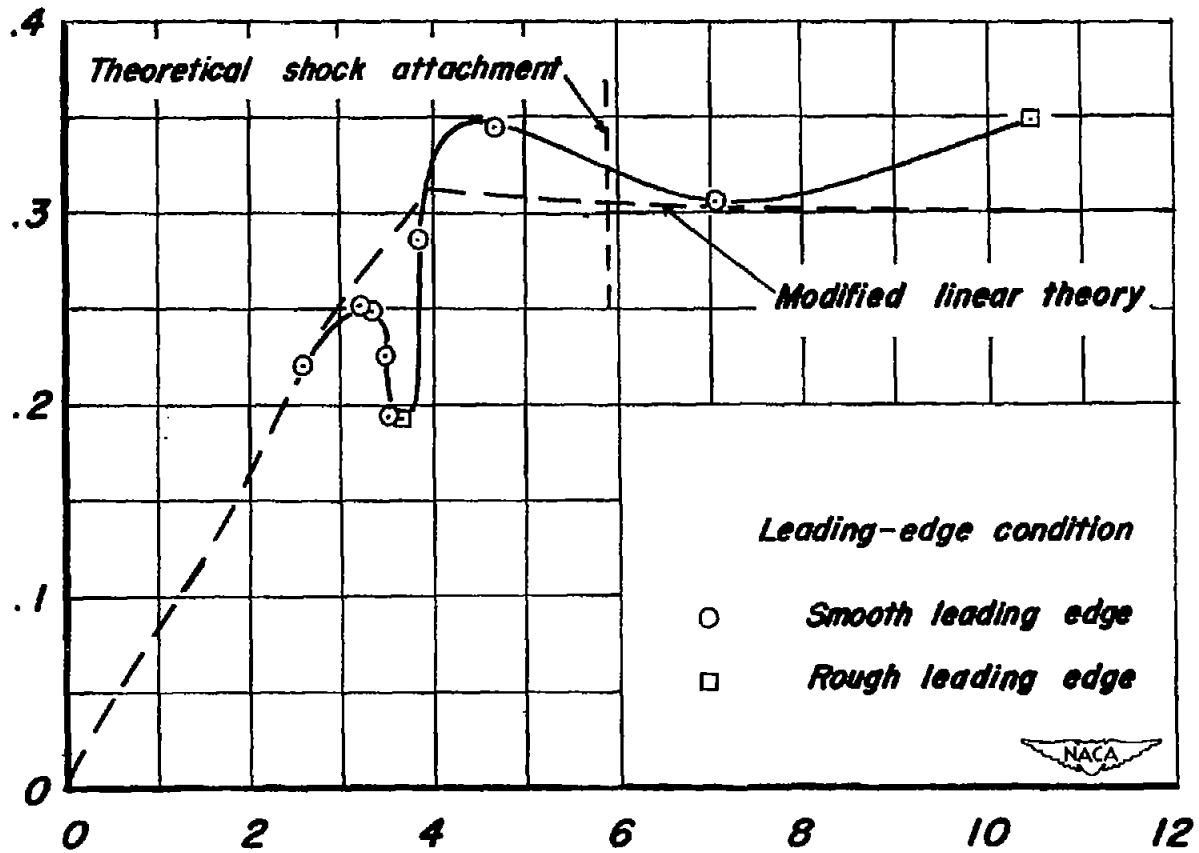

(c) Aspect ratio 2.31.

Figure 10.- Continued.

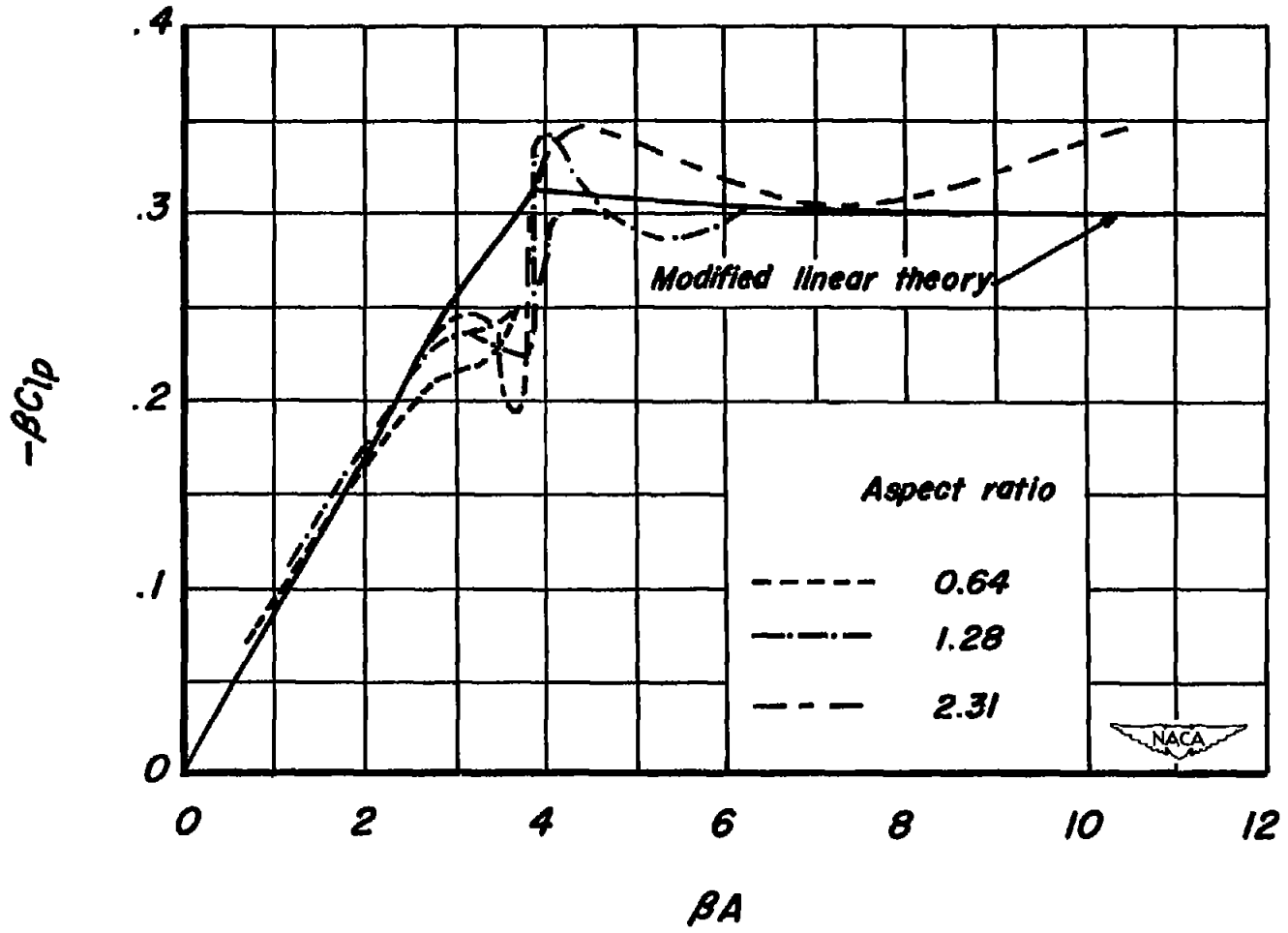

(d) Aspect ratios 0.64, 1.28 and 2.31.

Figure 10. - Concluded.

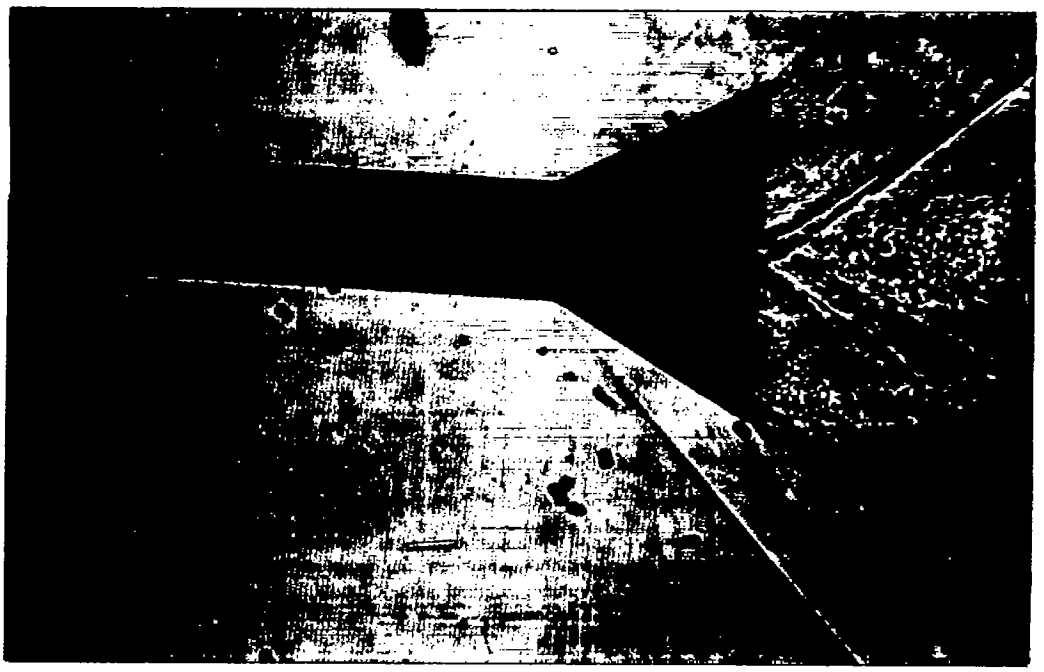

A-18818

(a) $\beta A = 2.60$, $\alpha = 3.50^\circ$

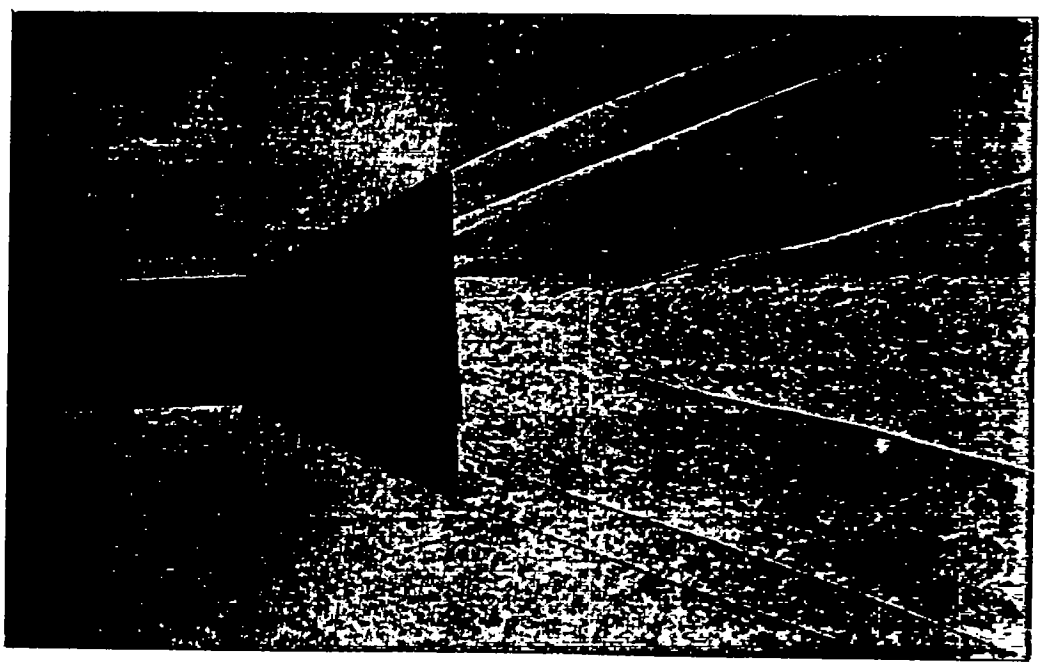

A-18819

(b) $\beta A = 7.07$, $\alpha = -2.75^\circ$

Figure 11.- Shadowgraphs of aspect ratio 2.31 models.

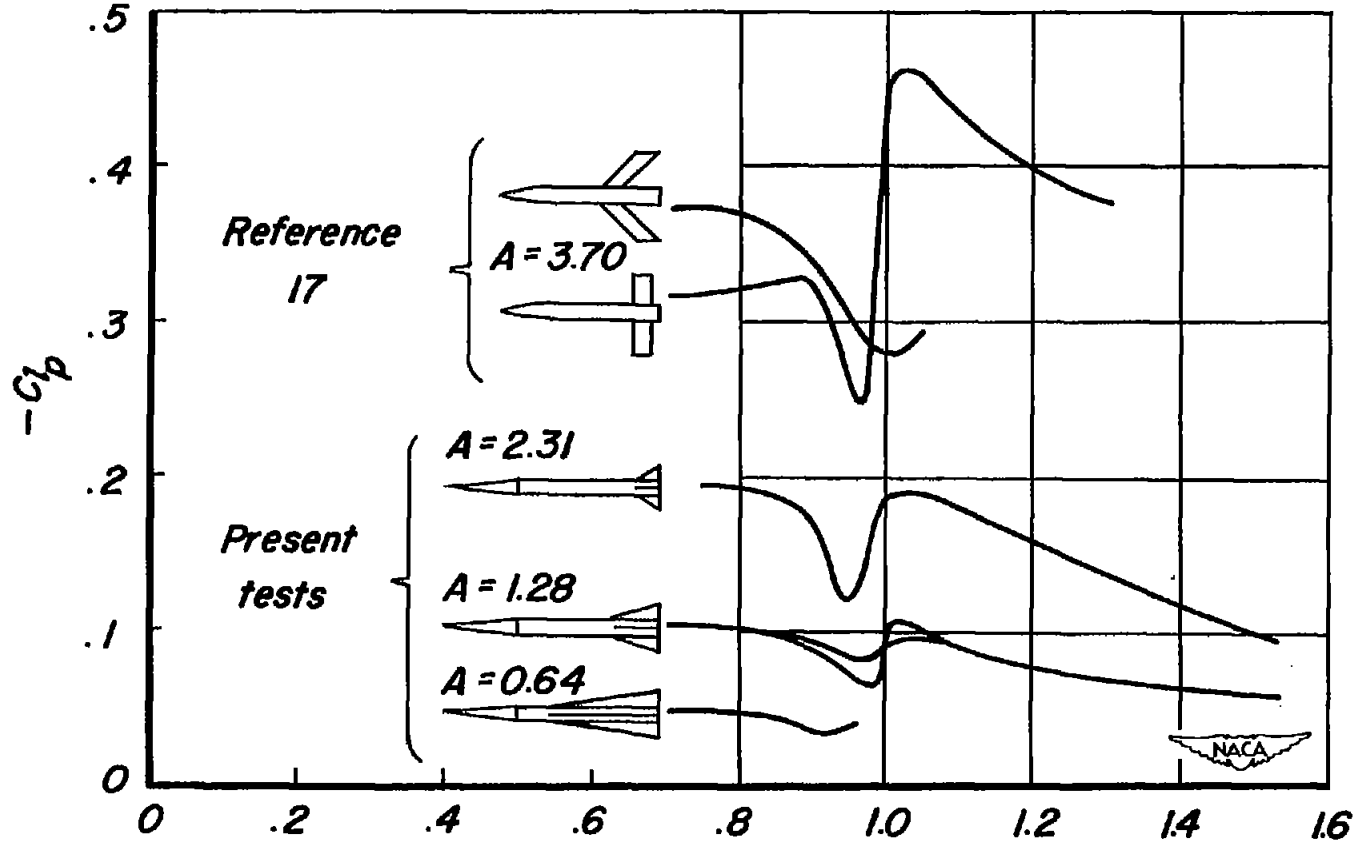

Figure 12.- Variation of the damping-in-roll coefficient of several wings with Mach number normal to the wing leading edge.

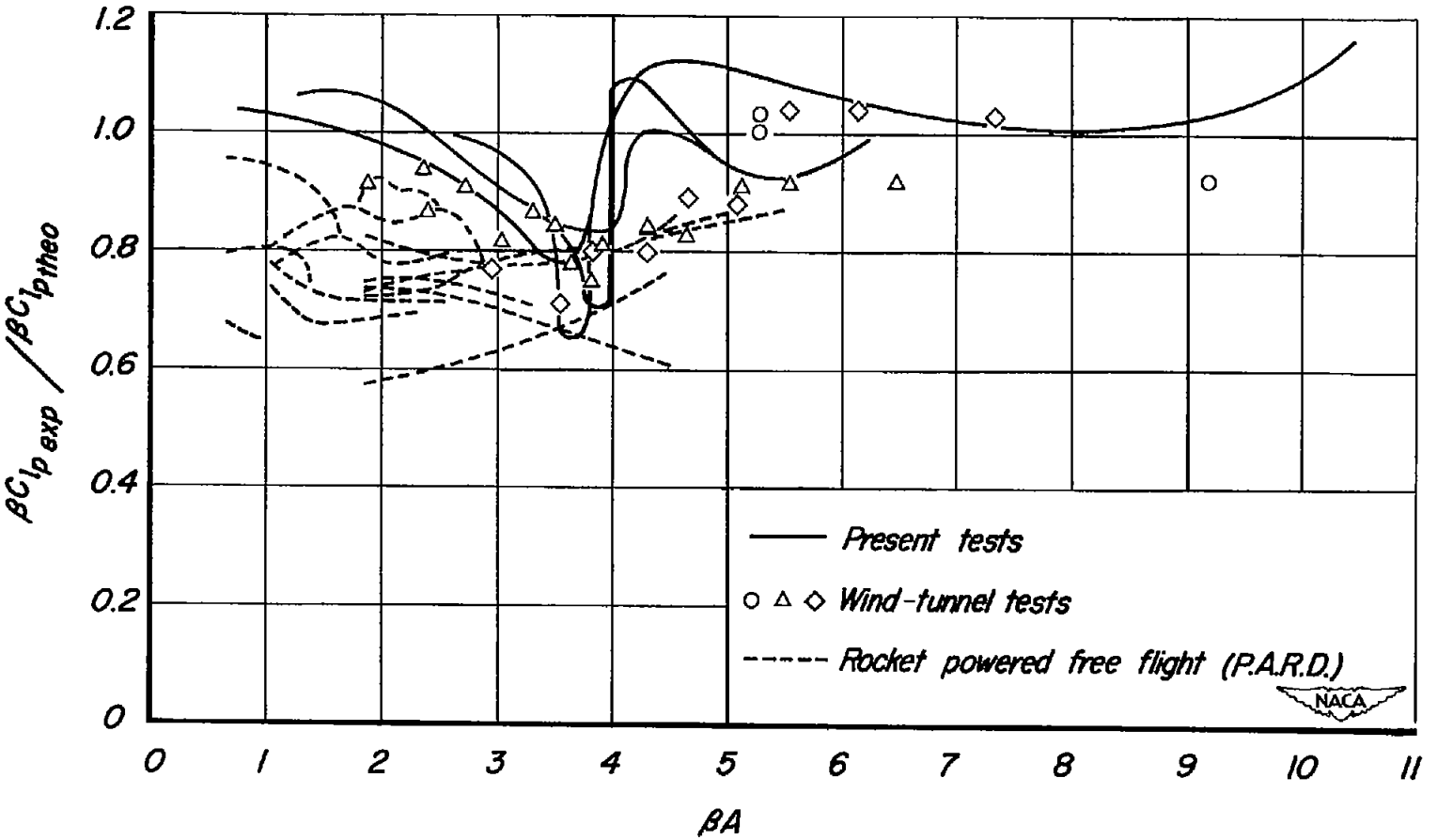

Figure 13.- Comparison of present data with those from other facilities on the damping in roll of triangular wings.

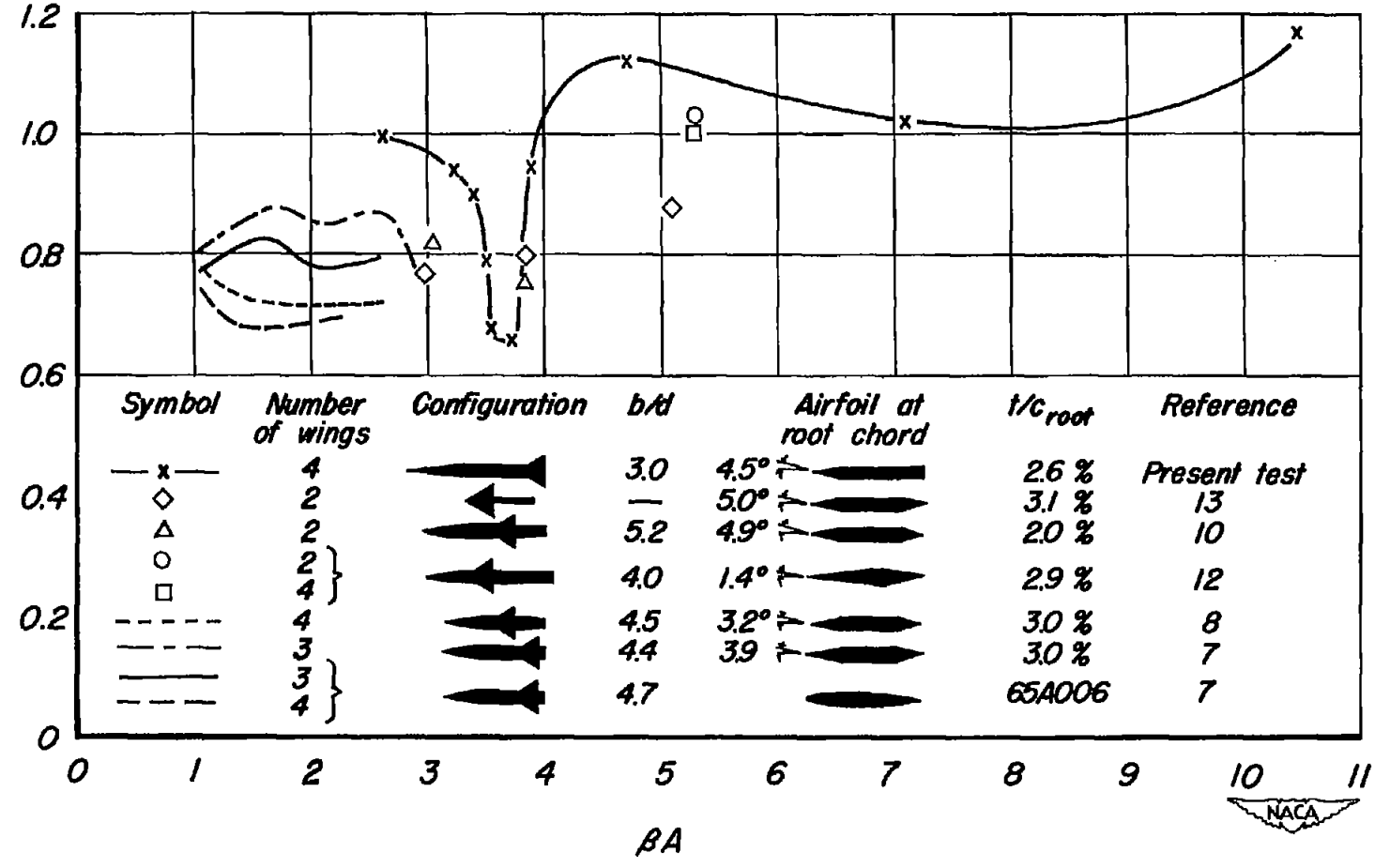

Figure 14.- Comparison of data for aspect ratio 2.31 wings.